



Interactions between Siglec-7/9 receptors and ligands influence NK cell–dependent tumor immunosurveillance

Camilla Jandus,¹ Kayluz Frias Boligan,¹ Obinna Chijioke,² He Liu,¹ Meike Dahlhaus,^{3,4} Thomas Démoulin,⁵ Christoph Schneider,¹ Marc Wehrli,¹ Robert E. Hunger,⁶ Gabriela M. Baerlocher,^{3,4} Hans-Uwe Simon,¹ Pedro Romero,⁷ Christian Münz,² and Stephan von Gunten¹

¹Institute of Pharmacology, University of Bern, Bern, Switzerland. ²Department of Viral Immunobiology, Institute of Experimental Immunology, University of Zurich, Zurich, Switzerland. ³Department of Hematology, University Hospital of Bern, Bern, Switzerland.

⁴Experimental Hematology, Department of Clinical Research, University of Bern, Bern, Switzerland.

⁵Institute of Virology and Immunoprophylaxis (IVI),Mittelhäusern, Switzerland. ⁶Department of Dermatology, University Hospital of Bern, Bern, Switzerland. ⁷Translational Tumor Immunology Group, Ludwig Center for Cancer Research at the University of Lausanne, Lausanne, Switzerland.

Alteration of the surface glycosylation pattern on malignant cells potentially affects tumor immunity by directly influencing interactions with glycan-binding proteins (lectins) on the surface of immunomodulatory cells. The sialic acid-binding Ig-like lectins Siglec-7 and -9 are MHC class I-independent inhibitory receptors on human NK cells that recognize sialic acid-containing carbohydrates. Here, we found that the presence of Siglec-9 defined a subset of cytotoxic NK cells with a mature phenotype and enhanced chemotactic potential. Interestingly, this Siglec-9⁺ NK cell population was reduced in the peripheral blood of cancer patients. Broad analysis of primary tumor samples revealed that ligands of Siglec-7 and -9 were expressed on human cancer cells of different histological types. Expression of Siglec-7 and -9 ligands was associated with susceptibility of NK cell-sensitive tumor cells and, unexpectedly, of presumably NK cell-resistant tumor cells to NK cell-mediated cytotoxicity. Together, these observations have direct implications for NK cell-based therapies and highlight the requirement to consider both MHC class I haplotype and tumor-specific glycosylation.

Introduction

Upon malignant transformation, sialic acid-containing carbohydrates (sialoglycans) can be aberrantly expressed by tumor cells as a result of genetic or epigenetic dysregulation of glycan synthesis pathways (e.g., glycosyltransferases) (1–4). Distinctly glycosylated tumor antigens on the cell surface or on secreted molecules (e.g., mucins) are diagnostically exploited as tumor markers (e.g., CA125, MUC1, CEA, and CA19-9). Sialoglycans influence many critical steps in tumor biology, including immunoeediting, tumor growth and proliferation, invasion, metastasis, and angiogenesis; in some instances, their presence has been correlated with poor patient survival (1, 2, 5–8).

NK cells act as first line of defense in tumor immunosurveillance (9). Distinct sialoglycan determinants are recognized as ligands to sialic acid-binding Ig-like lectin-7 (Siglec-7; also known as p75/AIRM1) and Siglec-9 receptors on human NK cells (10), which – similar to the classical inhibitory receptors CD94/NKG2A, killer Ig-like receptors (KIRs), and Ig-like transcripts (ILTs) – contain 1 or more immunoreceptor tyrosine-based inhibition motifs (ITIMs) in their cytoplasmic tail (11, 12). Recognition of MHC class I by inhibitory NK cell receptors provided the molecular basis of the “missing-self” hypothesis to explain the rejection of stressed, transformed, or infected cells that lack or downregulate cognate MHC class I molecules, and the associated capacity of NK cells to dis-

criminate between healthy self and target cells (13, 14). While in recent years, significant novel insights have accumulated on the role of MHC class I-specific inhibitory receptors in NK cell biology and tumor immunology (most notably in allogeneic hematopoietic stem cell transplantation for hematologic malignancies; ref. 9), comparably less is known about the role of MHC class I-independent ITIM-bearing receptors. Protection of tumor cells from innate immune attack can result from aberrant expression of sialoglycan ligands that engage the MHC class I-independent Siglec-7 and -9 receptors to govern NK cell inhibition.

NK cell subsets of humans consist of CD56^{dim} NK cells (CD56^{dim}CD16⁺KIR⁺), which represent about 90% of peripheral blood and spleen NK cells, express perforin and granzymes, and are the major cytotoxic subset (15, 16), and CD56^{bright} NK cells (CD56^{bright}CD16^{dim/-}KIR⁻), which constitute the majority of NK cells in lymph nodes and tonsils and, upon activation, primarily respond with cytokine production (17). Whereas Siglec-7 is known as a pan-NK cell marker (18, 19), Siglec-9 was recently reported to be selectively expressed in a subset of CD56^{dim} NK cells (20).

Siglecs comprise a lectin family of surface receptors that bind to sialoglycans and are predominantly expressed on cells of the hematopoietic system in a manner dependent on cell type and differentiation (21–24). Whereas sialic acid is ubiquitously expressed, typically at the terminal position of glycoproteins and -lipids, only very specific, distinct sialoglycan structures are recognized by individual Siglec receptors, depending on identity and linkage to sub-terminal carbohydrate moieties (22, 24). Knowledge about Siglec expression and function on NK cell subsets is still limited in terms of NK cell differentiation and maturation, and the role of Siglec

Authorship note: Camilla Jandus and Kayluz Frias Boligan contributed equally to this work.

Conflict of interest: The authors have declared that no conflict of interest exists.

Citation for this article: *J Clin Invest.* 2014;124(4):1810–1820. doi:10.1172/JCI65899.



ligand-receptor interactions in disease remains to be explored. Whether Siglec-7 and -9 ligands in human cancer are expressed on malignant or healthy cells is a subject of controversy (3, 25–28), as is the related question as to whether absence of inhibitory Siglec-ligand interactions promotes or inhibits tumor progression, either by uncoupled immune stimulation or by inhibition of immune defense (10, 25–27). Here, we found that Siglec-7 and -9 ligands were significantly overexpressed on a broad range of human malignant cells of different histological types and that surface Siglec-7 and -9 ligand expression determined cytotoxicity of human primary NK cells against both NK cell-susceptible and -resistant tumor cells. Given that Siglec-7 and -9, in analogy to KIRs, exist in humans but not in rodents (22), we performed *in vivo* experiments in mice with a reconstituted human NK cell compartment. Further in-depth analysis revealed that CD56^{dim}Siglec-9⁺ NK cells exhibited a more mature phenotype with distinct functional properties, such as enhanced chemotactic potential, and that the frequency of this subset was significantly reduced in the peripheral blood of cancer patients.

Results

Siglec-7 and -9 ligands are widely expressed on tumor cells of different histological origins. To determine the extent to which tumors express Siglec-7 and -9 ligands, we directly probed tumor cells and tissue sections using recombinant chimeras of Siglec molecules fused to human IgG1 Fc domains, as this strategy takes into account the spatial and complex cellular organization of sialoglycan ligands (29). High expression of Siglec-7 ligands was detected by flow cytometry on numerous cell lines, including HeLa cells and various leukemic (e.g., K562) and melanoma (e.g., A375) cells (Figure 1A). Staining for Siglec-9 ligands revealed an even broader expression profile, as high fluorescence signal intensities were detectable in the majority of tested cell lines, notably in those originating from hematologic malignancies and melanoma. In contrast to their malignant counterparts, Siglec-7 and -9 ligand expression in human PBMCs or primary melanocytes was low or undetectable (Figure 1A). Staining by a recombinant CD33-Fc fusion molecule was consistently negative in the tested cell lines (data not shown and Supplemental Figure 1A; supplemental material available online with this article; doi:10.1172/JCI65899DS1), thus excluding binding mediated by nonspecific Fc (IgG1). Confocal microscopic analysis of A375 melanoma cells revealed an intense cell surface-associated expression pattern, with only sparse intracellular staining for Siglec-7 and -9 ligands (Figure 1B). Binding of Siglec-7-Fc and Siglec-9-Fc fusion proteins was abrogated after enzymatic digestion of sialoglycans by neuraminidase (also known as sialidase) (30), thus confirming the sialic acid dependency of the staining. To confirm expression of Siglec-7 and -9 ligands in human malignancies, leukemic cells from patients with acute myeloid leukemia (AML) and chronic lymphocytic leukemia (CLL) were analyzed for Siglec-7 and -9 ligand expression by flow cytometry. Leukemic cells from all AML ($n = 3$) and CLL ($n = 3$) patients consistently stained highly double-positive for both Siglec-7 and -9 ligand expression (Figure 1C and Supplemental Figure 1B). To further confirm *in situ* expression of Siglec-7 and -9 ligands, immunohistochemistry on paraffin-embedded sections from human primary tumor specimens from melanoma, basal cell carcinoma (BCC), squamous cell carcinoma (SCC), and cutaneous T cell lymphoma (CTCL) patients was performed ($n = 3$ each; Figure 1D). Coexpression of Siglec-7 and -9 ligands was found in specimens from 5 of 6 melanoma patients and was restricted to

malignant cells. In contrast, no Siglec-7 or -9 ligand expression was found in the analyzed BCC, SCC, and CTCL specimens. Next, the melanoma cell-restricted expression of Siglec-7 and -9 ligands was further confirmed by confocal microscopy analysis. Melan-A-positive malignant melanoma cells displayed expression of Siglec-7 and -9 ligands, whereas staining of normal tissue was not detected in epidermal or dermal layers, nor in tumor-free skin sections (Figure 1E, Supplemental Figure 1, C–E, and data not shown), which indicated that the expression of Siglec-7 and -9 ligands in skin is confined to malignant cells.

Siglec-7 and -9 ligand expression protects tumor cells from NK cell responses. Next, we assessed the requirement of sialoglycan ligands to protect from NK cell lysis in cell lines with high (e.g., K562 and HeLa) or absent (e.g., 721.221) expression of Siglec-7 and -9 surface ligands. Desialylation by neuraminidase significantly enhanced cytolysis of NK cell-susceptible K562 cells by human peripheral blood NK cells *in vitro*, as measured in a ⁵¹Cr release assay (Figure 2, A and B). Similar results were obtained with HeLa cells (Figure 2, A and C), which indicated that desialylation even enhances the susceptibility of NK cell-resistant cells. In contrast, neuraminidase treatment had no effect on 721.221 cells (Figure 2A and Supplemental Figure 2). Consistent with these results, significant upregulation of the degranulation marker CD107a was found on NK cells exposed to desialylated K562 or HeLa target cells, but not to Siglec-7 and -9 ligand-negative 721.221 cells (Figure 2D). Intracellular synthesis of the cytokines IFN- γ and TNF- α and of the chemokine macrophage inflammatory protein-1 β (MIP-1 β) was increased in NK cells exposed to neuraminidase-treated K562 cells (Figure 2E and Supplemental Figure 3).

The sialome, defined as “total complement of sialic acid types and linkages and their modes of presentation on a particular organelle, cell, tissue, organ, or organism” (31), varies substantially among different species (22), and no orthologs or unambiguous functional paralogs for Siglec-7 or -9 exist in rodents (21). Therefore, we chose humanized NOD-SCID- $\gamma_c^{-/-}$ (huNSG) mice with a reconstituted human NK cell compartment (32) to test the tumor-protective role of sialoglycans *in vivo*. Circulating NK cells of huNSG mice expressed high levels of Siglec-7 (Supplemental Figure 4). Peritoneal injection of tumor cells in huNSG mice resulted in recruitment of human NK cells (human NKp46⁺, murine CD45⁻) within hours (data not shown). Before injection, neuraminidase-treated K562 or HeLa cells were labeled with lower CFSE concentrations compared with untreated controls, which allowed for discrimination between desialylated (low signal intensity) and nondesialylated (high signal intensity) tumor cells. Siglec-7 and -9 ligands on K562 cells were not reexpressed within 24 hours of neuraminidase treatment (Supplemental Figure 5). Desialylated and untreated K562 or HeLa cells were simultaneously injected at a 1:1 ratio into the peritoneal cavity of poly I:C-pretreated huNSG mice (32). Flow cytometric analysis of the peritoneal lavage as early as 12 hours after injection revealed a decrease in the total numbers of K562 and HeLa cells (29.8% and 41.8% decreases, respectively). The loss of cells was much more pronounced among desialylated tumor cells, as concomitantly a higher percentage of untreated, fully glycosylated tumor cells was recovered (Figure 2F).

To further substantiate a tumor-protective role of Siglec-7 and -9 ligands, we generated Fab fragments from mAbs against Siglec-7 (clone Z176) and Siglec-9 (clone E10-286) to specifically block ligand-receptor interactions. Anti-Siglec-7 and anti-Siglec-9 Fabs at 5 μ g/ml led to substantially enhanced NK cell cytotoxicity against K562 and

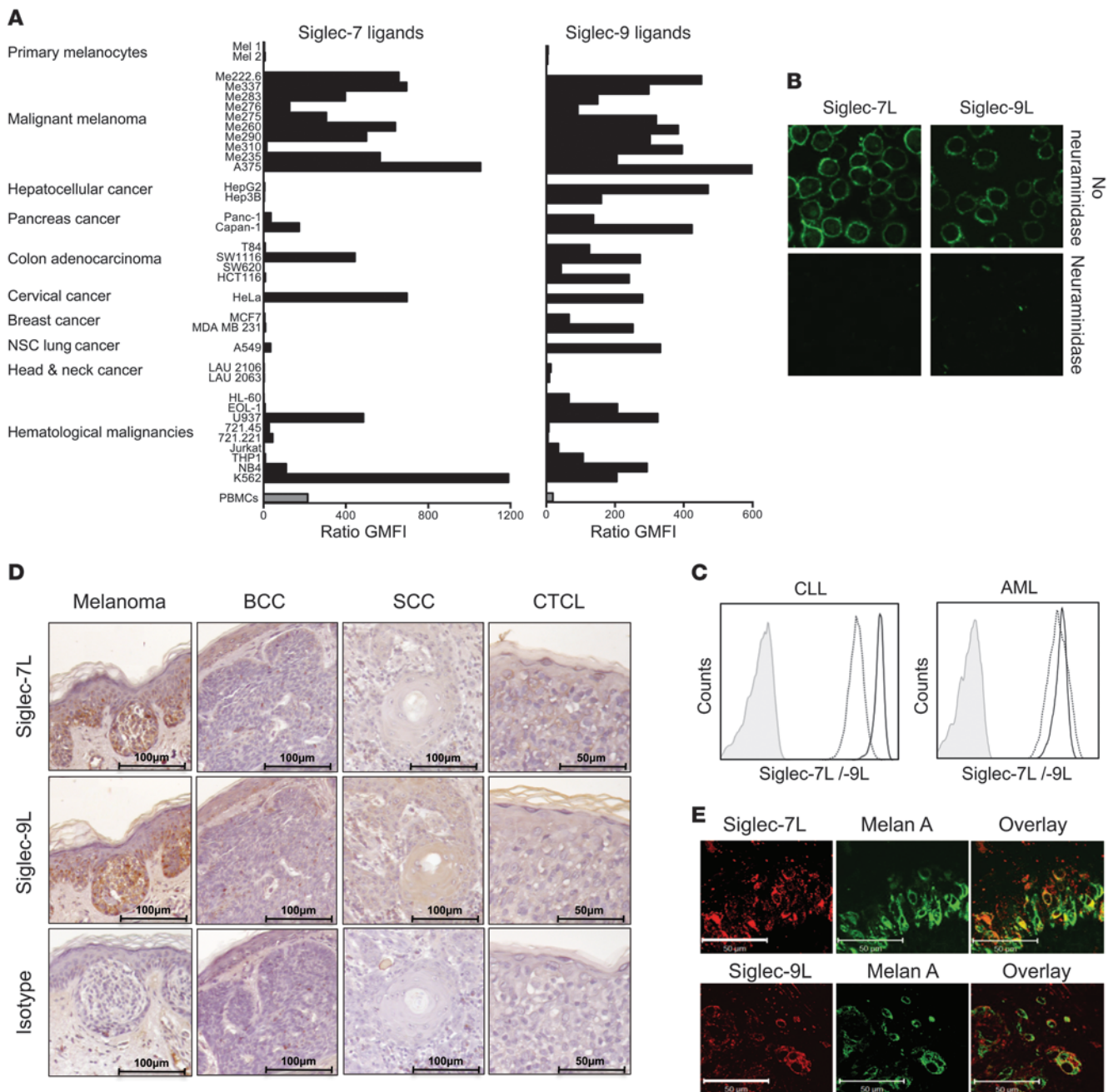


Figure 1

Human tumor cells express variable, but significant, levels of Siglec-7 and -9 ligands. (A–C and E) Immunofluorescence binding studies by flow cytometry (A and C) or immunofluorescence confocal microscopy (B and E) using recombinant Siglec-Fc (human IgG1) fusion proteins coupled to secondary PE-conjugated (Fab')₂ goat anti-human Fc antibody. (A) Broad analysis of ligand expression to Siglec-7 and -9 on different tumor cell lines, as well as on primary melanocytes (n = 2) and PBMCs (n = 9) from healthy donors for comparison. Values are expressed as geometric mean fluorescence intensity (GMFI) ratio of specific staining compared with secondary antibody only. (B) Expression of Siglec-7 and -9 ligands on A375 melanoma cells was localized to the cell surface. Staining was lost upon neuraminidase treatment (sialic acid dependency). Original magnification, ×630. (C) Expression levels of Siglec-7 and -9 ligands on CLL and AML cells, as revealed by flow cytometric analysis. Histograms are representative of 3 CLL and 3 AML patients. (D) Lectin immunohistochemistry for Siglec-7 and -9 ligand expression in paraffin-embedded tissues representative of melanoma, BCC, SCC, and CTCL sections. Scale bars: 100 μm (melanoma, BCC, and SCC); 50 μm (CTCL). (E) Paraffin-embedded primary tissue biopsy sections of malignant melanoma lesions in epidermal skin layers, costained for the melanoma marker Melan-A and Siglec-7 or Siglec-9 ligands. Scale bars: 50 μm. Data are representative of at least 2 (B), 3 (D), or 5 (E) independent experiments.

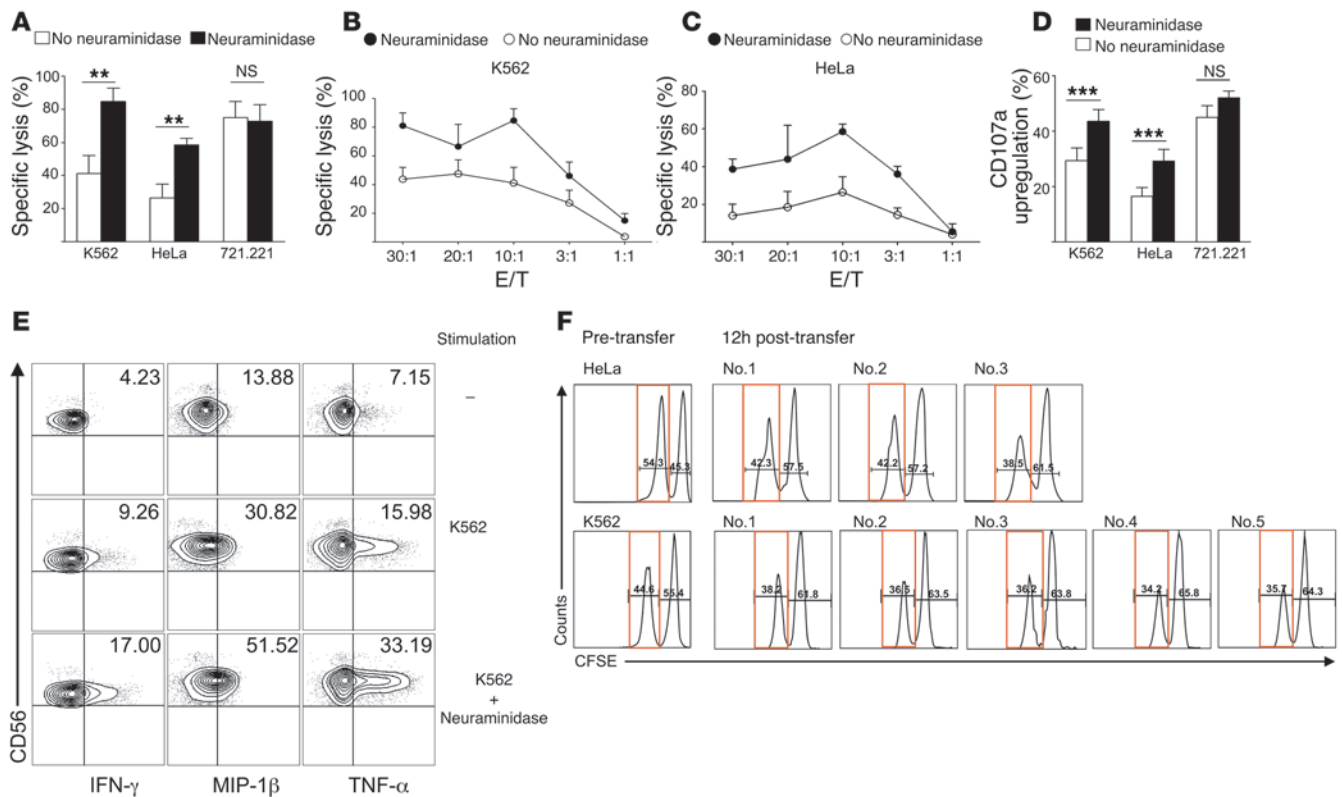


Figure 2

Desialylation of target cells that express ligands of Siglec-7 and -9 enhances NK cell cytotoxicity and cytokine secretion. (A–C) Cytotoxicity of isolated peripheral blood NK cells from healthy donors against K562 (A and B), HeLa (A and C), and 721.221 (A) cell lines, assessed in a ⁵¹Cr release assay, without or with neuraminidase treatment of target cells. Cytotoxicity was evaluated at a 10:1 E/T ratio (A) or as indicated (B and C). (D) Flow cytometric CD107a measurement on NK cells after coculture with desialylated or untreated K562, HeLa, or 721.221 cells at a 1:1 E/T ratio. (E) Intracellular cytokine measurement in NK cells in the presence of K562 cells with or without neuraminidase treatment (10:1 E/T ratio). (F) Flow cytometry of CFSE-labeled HeLa and K562 cells, prior to intraperitoneal injection (Pre-transfer) and after recovery 12 hours later in individual poly I:C–preactivated huNSG mice (no. 1–3 for HeLa; no. 1–5 for K562). Percentage of CFSE^{hi} (wild-type K562 and HeLa) and CFSE^{lo} (desialylated K562 and HeLa; red boxes) cells is indicated. ***P* < 0.005, ****P* < 0.001, Student’s *t* test. Data are representative of at least 5 (A–C), 7 (D), 4 (E), and 2 (F) independent experiments.

HeLa cells, but not against 721.221 cells (Figure 3A), the latter of which expressed neither Siglec-7 nor -9 ligands (see above). The permissive effect of anti-Siglec-7 and anti-Siglec-9 Fabs was observable at different effector/target (E/T) ratios (Figure 3, A–C), but blocking Siglec-9 was slightly less efficient compared with blocking Siglec-7 (Figure 3A), consistent with the lower frequency and reduced killing capacity of CD56^{dim}Siglec-9⁺ NK cells. The combination of Fab fragments of Siglec-7 and -9 had no additive effect in potentiating NK cell cytotoxicity (Supplemental Figure 6), likely because both of these structurally related receptors target similar intracellular signaling pathways. We also used intact mAbs to exploit their agonistic action, which has been demonstrated in previous studies (18, 33). NK cell cytotoxicity was inhibited by ligation of Siglec-7 and -9 by intact anti-Siglec-7 and anti-Siglec-9 mAbs (Z176 and E10-286, respectively), but not by the null clone 191240 against Siglec-9 (Figure 3C and Supplemental Figure 7A). Anti-Siglec-9 did not affect the cytotoxic activity of sorted CD56^{dim}Siglec-9⁻ NK cells (Supplemental Figure 7B). Anti-Siglec-7 and, to a lesser extent, anti-Siglec-9 mAbs inhibited CD107a upregulation and IFN- γ secretion of NK cells, but had no effect on their survival or proliferation (Figure 3, D and E, and Supplemental Figure 7, C and D).

Siglec-9 defines a subset of mature cytotoxic CD56^{dim} NK cells with enhanced chemotactic potential. Next, we set out to phenotypically and functionally characterize human primary NK cells expressing Siglec-7 and -9, and eventually to identify other Siglecs involved in modulating the effector function of NK cells. Human peripheral blood NK cells were screened by flow cytometry, which demonstrated the exclusive presence of Siglec-7 and -9 on NK cell surfaces (Supplemental Figure 8A). This observation was confirmed after neuraminidase treatment (Supplemental Figure 8A), to remove potentially “masking” sialoglycans bound in cis on the same cell membrane (21). Whereas Siglec-7 was ubiquitously distributed in the NK cell compartment, Siglec-9 was absent on CD56^{bright} NK cells, but selectively expressed on about 40%–50% of CD56^{dim} NK cells, 10%–20% of which was masked, as revealed by neuraminidase treatment (Supplemental Figure 8B). Surface expression of Siglec-9 on total NK cells or fluorescence-activated cell sorted CD56^{dim}Siglec-9⁺ NK cell subsets was not influenced by exposure to the cytokines IL-2, IL-8, IL-12, IL-15, IL-18, or IL-21, alone or in combination, nor did these cytokines induce Siglec-9 expression in Siglec-9⁻ subsets (Supplemental Figure 8, C and D, and data not shown).

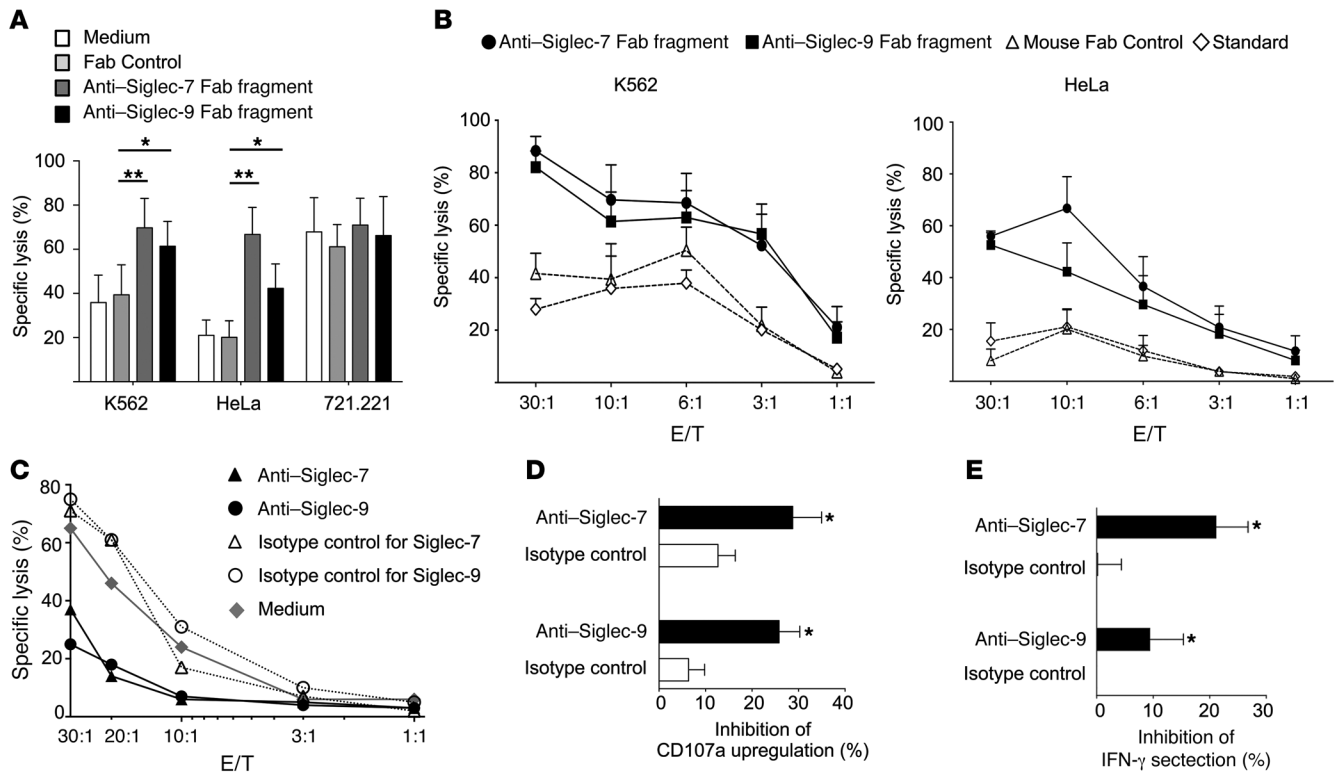


Figure 3

NK cell responses are attenuated after engagement of Siglec-7 and -9 by ligands on tumor cells or targeting with agonistic mAbs. (A and B) Cytotoxicity of isolated peripheral blood NK cells from healthy donors against K562, HeLa, and 721.221 cells in the presence of blocking anti-Siglec-7 (clone Z176) and anti-Siglec-9 (clone E10-286) Fab fragments at 10:1 E/T ratios (A) or as indicated (B), as assessed in a ⁵¹Cr-release assay. (C) Cytotoxicity of isolated peripheral blood NK cells from healthy donors against K562 cells in the presence or absence of intact anti-Siglec-7 or anti-Siglec-9 agonistic mAbs at the indicated E/T ratios, as assessed in a ⁵¹Cr release assay. (D) Flow cytometric CD107a measurement on NK cells, in the presence or absence of intact anti-Siglec-7 or anti-Siglec-9 mAbs. (E) Inhibition of IFN-γ secretion after activation of NK cells with IL-12 and IL-18, in the presence or absence of the indicated intact mAbs. *P < 0.05, **P < 0.005, Student's t test. Data are representative of at least 5 (A and B), 10 (C), or 6 (D and E) independent experiments.

Upon release from the bone marrow, human immature CD56^{bright} NK cells may undergo differentiation to CD56^{dim} NK cells in the periphery, a process that is paralleled by the acquisition (e.g., increasing number of KIRs, CD57) or loss (e.g., NKG2A, CD27) of distinct and characteristic molecules (34, 35). CD27, a molecule expressed by naive cells, was not detectable in the CD56^{dim}Siglec-9⁺ subset; inversely, markers that typically define mature cells, like CD57 and KLRG1, were significantly upregulated in CD56^{dim}Siglec-9⁺ cells compared with the CD56^{dim}Siglec-9⁻ subset (Figure 4A). Expression of the activation marker CD69 was higher on CD56^{dim}Siglec-9⁺ cells, whereas no difference in CD25 expression was observed (data not shown).

To assess the replicative history of these NK cell subsets, we measured telomere length in CD56^{bright}, CD56^{dim}Siglec-9⁺, and CD56^{dim}Siglec-9⁻ NK cells isolated from the peripheral blood of 3 healthy donors using automated multicolor flow-FISH (see Methods). Consistent with being less mature, CD56^{bright} cells showed a trend for longer telomeres than CD56^{dim} NK cells (mean, 5.00 ± 0.58 kb versus 4.56 ± 0.41 kb; P = 0.220; Figure 4B). In contrast, CD56^{dim}Siglec-9⁺ and CD56^{dim}Siglec-9⁻ NK cells had similar mean telomere lengths (4.56 ± 0.51 and 4.55 ± 0.39 kb, respectively).

Next, we used flow cytometry to compare the expression of Siglec-7 and -9 on NK cells in human cord blood and adult peripheral blood. Even without unmasking by neuraminidase treatment, cord blood CD56^{bright} NK cells stained consistently Siglec-7⁺, whereas adult peripheral blood cells exhibited broader staining variability (Figure 4, C and D). Expression levels of Siglec-7 and -9 were higher on cord blood CD56^{dim} NK cells compared with their adult counterparts, and 40% of untreated and 60% of neuraminidase-treated cells were Siglec-9⁺. Upon neuraminidase treatment, about 10% of CD56^{bright} NK cells from cord blood were Siglec-9⁺. Together, these results suggested that acquisition of Siglec-9 is an early event upon differentiation from CD56^{bright} to CD56^{dim} NK cells, while its expression is either transient or stabilized in a subset of cells reaching full maturation.

CD56^{dim}Siglec-9⁺ NK cells exhibited a significantly reduced cytotoxic capacity against K562 target cells compared with CD56^{dim}Siglec-9⁻ NK cells (Figure 5A), which we eventually attributed to the elevated expression of inhibitory receptors (e.g., KIRs and ILT2) found on these cells (Figure 5, B and C). In contrast, expression of the activating receptor NKG2D and the natural cytotoxicity receptors (NCRs) NKp46 and NKp30 was similar between the CD56^{dim}Siglec-9⁺ and CD56^{dim}Siglec-9⁻ NK cell subsets (Supplemen-

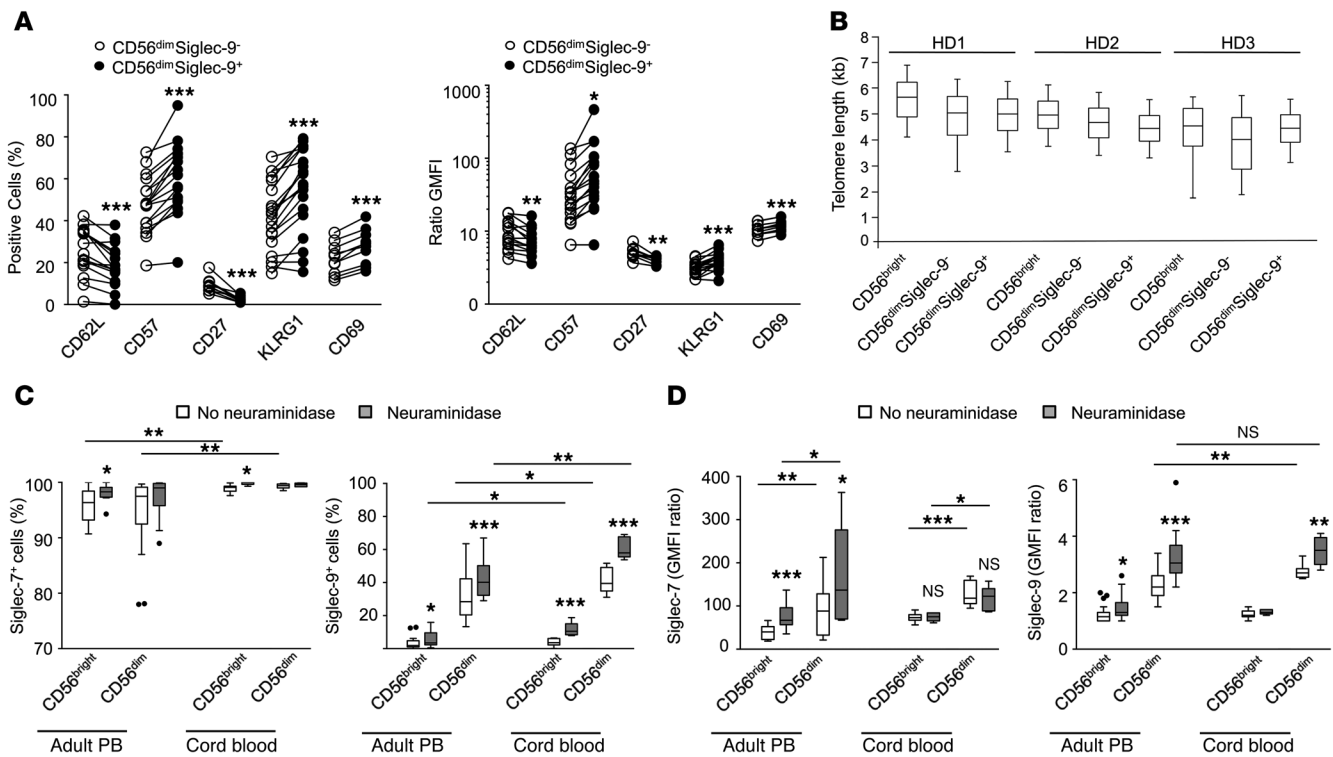


Figure 4 Siglec-9 defines a subset of NK cells with a more mature phenotype, yet similar telomere length, present in adult and cord blood. **(A)** Flow cytometry for surface expression of adhesion and activation markers. Shown are frequency and GMFI ratio of specific staining to isotype-matched control. **(B)** Telomere length analysis of different NK cell subsets from 3 healthy donors (HD). 50th percentile is shown as lines within boxes and numerals; upper and lower margins of the boxes denote 25th and 75th percentile; whiskers denote 5th and 95th percentile. **(C and D)** Siglec-7 and -9 expression among NK cell subsets in adult peripheral blood (PB; $n = 14$ [Siglec-7], 27 [Siglec-9]) and cord blood ($n = 9$). * $P < 0.05$, ** $P < 0.005$, *** $P < 0.001$, Student's t test.

tal Figure 9). CD56^{dim}Siglec-9⁺ NK cells exhibited higher expression of the chemokine receptors CXCR1 and CX3CR1, while the receptors CXCR3, CCR5, and CCR7 were virtually absent (Figure 5, E and F). Since the most striking difference between CD56^{dim}Siglec-9⁺ and CD56^{dim}Siglec-9⁻ NK cells was found for CXCR1, we compared their relative chemotactic capacity toward a gradient of the CXCR1 ligand IL-8, a known chemoattractant for NK cells (36, 37). Highly pure fluorescence-activated cell sorted CD56^{dim}Siglec-9⁺ and CD56^{dim}Siglec-9⁻ NK cells were stimulated to migrate to a gradient of 1 nM recombinant human IL-8 (rhIL-8). Concordantly with the higher CXCR1 expression, CD56^{dim}Siglec-9⁺ NK cells exhibited a significantly higher propensity for chemotaxis toward IL-8 (Figure 5D).

CD56^{dim}Siglec-9⁺ NK cells are reduced in peripheral blood of cancer patients. Given the peculiar characteristics of the CD56^{dim}Siglec-9⁺ NK cell subset and the well-established role of NK cells in anti-tumor immune responses (9), we next determined whether NK cells isolated from peripheral blood from cancer patients display altered occurrence of NK cell subsets or expression levels of Siglec-7 and -9 receptors. Compared with healthy donors ($n = 22$), absolute numbers of total NK cells among PBLs were similar in patients with colon adenocarcinoma (CoACA; $n = 10$) or malignant melanoma ($n = 11$) (Supplemental Figure 10A). Furthermore, no difference in terms of the cytolytic capacity of NK cells was observed between NK cells from melanoma patients and healthy donors (Supplemental Figure 10B). For flow cytometric analysis of

Siglec-7 and -9, NK cells were analyzed with or without neuraminidase pretreatment to exclude masking effects by bound sialoglycan ligands. Siglec-7 was expressed at similar levels on peripheral blood NK cells of cancer patients and healthy donors (Supplemental Figure 10C). Interestingly, both positivity and expression levels of Siglec-9 among peripheral blood CD56^{dim} NK cells were significantly reduced in the malignant melanoma and CoACA patients compared with healthy donor controls (Figure 6, A and B). Neuraminidase treatment enhanced the staining, which suggests that Siglec-9 receptors are partially masked by bound sialoglycans. However, Siglec-9 staining after unmasking by enzymatic treatment remained lower in NK cells of cancer patients, which confirmed that the expression of this surface receptor is reduced in cancer. The reduced occurrence of CD56^{dim}Siglec-9⁺ NK cells in peripheral blood of cancer patients might eventually be associated with the enhanced chemotactic properties of this subset (migration), but is likely attributable to other, yet-unknown factors, including cell-specific characteristics.

Discussion

Altered surface glycosylation with overexpression of sialoglycans that engage inhibitory Siglec receptors on NK cells may provide a general mechanism to shield tumor cells from innate immunity. By this strategy, tumor cells might counter NK cell activation, after loss of MHC class I expression (missing-self) and disengagement

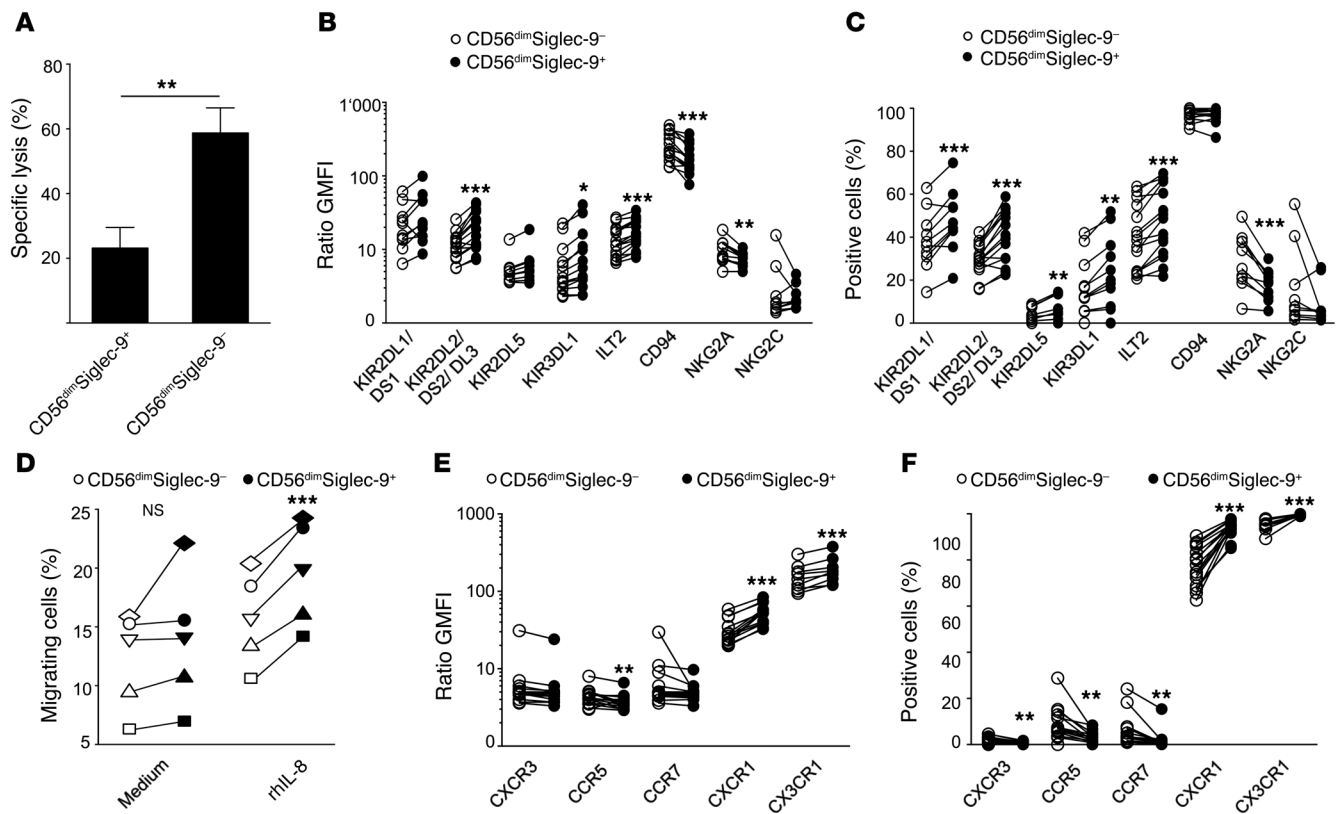
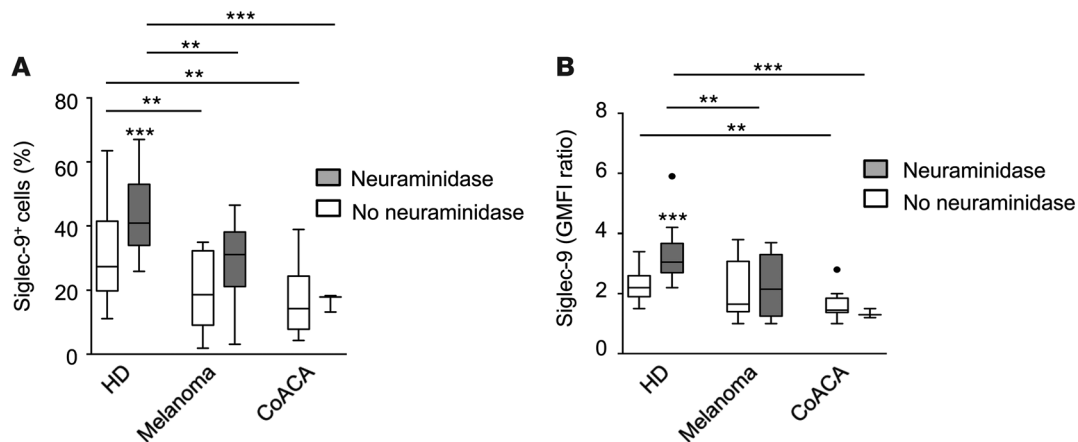


Figure 5 CD56^{dim}Siglec-9⁺ NK cells are less cytotoxic, yet exhibit features of enhanced chemotactic propensity. (A) Cytotoxic capacity of sorted CD56^{dim}Siglec-9⁺ and CD56^{dim}Siglec-9⁻ NK cells against K562 cells (n = 7). (D) Migration of sorted CD56^{dim}Siglec-9⁺ and CD56^{dim}Siglec-9⁻ NK cells to medium or medium supplemented with 1 nM rhIL-8 (n = 5). (B, C, E, and F) Flow cytometry for surface expression of inhibitory receptors (B and C) and of maturation, adhesion, and activation markers (E and F). Shown are frequency (C and F) and GMFI ratio of specific staining to isotype-matched control (B and E). *P < 0.05, ***P < 0.001, Student's t test.

of classical inhibitory NK receptors, by interacting with alternative ITIM-containing – but MHC-independent – Siglec receptors. Our present findings revealed that sialic acid-containing ligands of the human inhibitory NK cell receptors Siglec-7 and -9 were widely expressed on tumor cells of different histological origin. Expression of Siglec-7 and -9 ligands protected malignant cells from attack by NK cells in vitro and in an in vivo model, using mice with a reconstituted human NK cell compartment. Interference with Siglec-ligand interactions conferred substantially increased NK cell cytotoxicity, not only against NK cell-susceptible K562 tumor cells, but also against NK cell-resistant cells. Depending on their differential expression on tumor cells, Siglec ligands might preferentially interact with the pan-NK cell receptor Siglec-7 or with Siglec-9, which was expressed on a mature subset of cytotoxic CD56^{dim} NK cells with enhanced chemotactic potential. This CD56^{dim}Siglec-9⁻ NK cell subset was found to be reduced in the peripheral blood of cancer patients.

The importance of directly studying the sialome on the intact cell or tissue, taking into account the spatial and complex cellular organization of sialic acid, has recently been highlighted (29). Therefore, we directly probed tumor cells and tissue sections for detection of Siglec ligands using recombinant soluble chimeras of Siglec molecules fused with the Fc portion of human IgG1. Such pseudoantibodies have been suggested to be powerful tools for

detecting specific types and arrangements of sialic acids in situ (1). Given the broad Siglec-7 and -9 binding to different tumor types, it is conceivable that future pull-down assays using Siglec-Fc fusion proteins might lead to the identification of further physiological or pathophysiological Siglec ligands and, importantly, of novel tumor markers and tumor-specific targets for therapy. Candidate ligands are tumor-related mucins that contain predominantly Ser- or Thr-linked (O-linked) oligosaccharides, including sialoconjugate tumor antigens (e.g., STN). Indeed, MUC16 has recently been identified as a ligand for Siglec-9 (20). Cell surface MUC16 is overexpressed by human epithelial ovarian tumors, and shed MUC16 can be detected in peritoneal fluid or serum as the tumor marker CA125. Other candidate ligands are gangliosides, which are known to be highly expressed in a broad variety of tumor types (2) and have been reported to be specifically bound by Siglec-7 and -9 (38, 39). Notably, the gangliosides GD3, GD2, and GT1b are found predominantly on human tissue and tumor cells of neuroectodermal origin and constitute ligands for Siglec-7 and -9, which in our analysis exhibited strong binding to melanoma cell lines or melanoma lesions in situ as well as to primary leukemic cells of patients with AML or CLL. Enhanced expression of the ganglioside GD3 in GD3 synthase-transfected P815 cells strongly bound to recombinant Siglec-7-Fc protein, but caused enhancement (rather than inhibition) of NK cell cytotoxicity, due

**Figure 6**

The CD56^{dim}Siglec-9⁺ NK cell subset is reduced in the peripheral blood of cancer patients. (A and B) Expression of Siglec-9 on peripheral blood NK cells of healthy donors ($n = 22$) or patients with melanoma ($n = 11$) or CoACA ($n = 10$). Shown are frequency (A) and GMFI ratio of specific staining to isotype-matched control (B), with or without neuraminidase treatment. Lines within boxes denote 50th percentile; upper and lower margins of the boxes denote 25th and 75th percentile; whiskers denote 5th and 95th percentile. * $P < 0.05$, ** $P < 0.005$, *** $P < 0.001$, Student's t test.

to Siglec-7-independent effects (10). The ganglioside DSGb5 was reported to be expressed on renal carcinoma cells and to serve as a ligand for Siglec-7 (27). GD3 or DSGb5 expression alone had no effect on untreated NK cells, and pretreatment of NK cells with neuraminidase was required to inhibit NK cell cytotoxicity, probably by unmasking Siglec-7 (10, 27). In contrast to these reports, we showed here that unmodified expression of Siglec-7 or -9 ligands on malignant cells of distinct types of cancer was strong enough to directly inhibit antitumor responses of human primary NK cells. Hence, multiple heterogeneous putative ligands for Siglec-7 and -9 exist, and quantitative and qualitative differences in distinct tumor types appear to determine their protective capacity against NK cell-mediated immune responses.

To date, no detailed phenotypical analysis comparing CD56^{dim}Siglec-9⁺ and CD56^{dim}Siglec-9⁻ NK cells has been performed. Hence, the abundant expression of Siglec-9 ligands on tumor cells prompted us to phenotypically and functionally analyze this NK cell subset. We found that CD56^{dim}Siglec-9⁺ NK cells exhibited a more mature phenotype, with higher expression levels of inhibitory KIRs and ILT2 receptors and concomitantly reduced – but still preserved – cytotoxic capacity to kill K562 target cells. In contrast, the chemotactic potential of CD56^{dim}Siglec-9⁺ NK cells to migrate toward IL-8 was superior to that of CD56^{dim}Siglec-9⁻ NK cells, and surface expression levels of the chemokine receptors CXCR1 (IL-8 receptor) and CX3CR1 was higher on this subset. Based on telomere length, CD56^{dim} NK cells had undergone approximately 5–10 more cell divisions than CD56^{bright} NK cells, assuming an average telomere shortening of 50–100 bp per cell division (40). Interestingly, we found no difference in telomere length between the CD56^{dim}Siglec-9⁺ and CD56^{dim}Siglec-9⁻ NK cell subsets, despite the observed phenotypically fully mature state of peripheral blood CD56^{dim}Siglec-9⁺ NK cells. These findings are indicative of a proliferation-independent role of Siglec-9 as a maturation marker. The frequency of CD56^{dim}Siglec-9⁺ NK cells was higher in cord blood compared with adult peripheral blood, and neuraminidase treatment demonstrated that CD56^{dim}Siglec-9⁺ NK cells comprised even the majority of cord blood CD56^{dim} NK cells. These data suggest that acquisition of

Siglec-9 is an early event upon differentiation from CD56^{bright} to CD56^{dim} NK cells, but expression of the receptor might be transient and only stabilized in cells that undergo full maturation, while being lost in activated short-lived NK cells. It has been proposed that immunological parameters in cancer could be used as a prognostic factor (41). Indeed, immunological scores have been reported as a better predictor of patient survival than contemporary histopathological methods used to stage colorectal cancer (42). In this regard, our observation that the frequency of CD56^{dim}Siglec-9⁺ NK cells and Siglec-9 expression levels were reduced in the peripheral blood of malignant melanoma and CoACA patients warrants future clinical studies. Detailed analysis of patient samples at different stages of disease might test the suitability of Siglec-9 expression as a biomarker and provide explanations for the decreased occurrence of CD56^{dim}Siglec-9⁺ NK cells in cancer.

Our findings indicate that targeting Siglec-7 and -9 on NK cells, or their ligands on malignant cells, might prove an attractive strategy by which to broaden indications or to implement current strategies for NK cell-based therapy to augment antitumor immunity (43). The observation that NK cells were able to overcome the resistance of presumably NK cell-nonsusceptible tumor cells suggests that this approach may expand the range of indications for NK cell-based strategies. Manipulation of inhibitory receptors has been recently exploited in the context of both innate (e.g., NK cells) and adaptive (e.g., CD8⁺ T cells) immunity to enhance antitumor activity. In both preclinical models and clinical trials of cancer patients, blockade of KIRs as well as interference with CTLA-4 or PD-1 provided solid *in vivo* evidence that modulation of the balance between inhibitory and activating signals in both adaptive and innate immune cells might represent an attractive strategy for combating hematologic malignancies as well as solid tumors (43–47). Similarly, it might be speculated that the clinical efficacy of allogeneic KIR-mismatched human stem cell transplants in the clinical setting of leukemic diseases might be further enhanced by blockade of Siglec-7 and -9 on donor NK cells (48). Inversely, agonistic triggering of Siglec-7 and -9 as inhibitory NK cell receptors might prove promising in the context of reducing graft failure in certain types of solid organ transplantation (49). The cell type-restricted,



differentiation-dependent expression pattern of Siglecs renders them attractive targets for functional targeting with agonists/antagonists or in cell-based therapies (23, 50, 51). Siglecs, in particular Siglec-2, -3, and -8 (CD22, CD33, and Siglec-F, respectively, in the murine system) have been successfully targeted with different approaches in preclinical models of autoimmune and allergic disorders, or, for the treatment of certain types of leukemia, in both preclinical and clinical trials (e.g., AML, non-Hodgkin lymphoma, and hairy cell leukemia) (23, 50). Our results provide insights into Siglec-7 and -9 receptor-ligand interactions in malignancy that may form the basis for novel therapeutic approaches and identification of novel diagnostic and prognostic biomarkers in human cancer.

Methods

Cells and tissues. Blood from healthy subjects was collected upon informed consent, or buffy coats were purchased from the Blood Transfusion Centres of Bern and Lausanne, Switzerland. Cord blood samples were obtained from umbilical cord veins immediately after delivery of the placenta (University Hospital of Lausanne, Lausanne, Switzerland, and University Hospital of Ghent, Ghent, Belgium). Peripheral blood was obtained from melanoma, CoACA, AML, and CLL patients. Archived tissue samples of melanoma, BCC, SCC, and CTCL between the years 2001 and 2006 from patients at the Department of Dermatology of Inselspital (Bern, Switzerland) were included in this study. Mononuclear cells were obtained by density centrifugation using Ficoll-Hypaque solution (Biochrom AG). For functional experiments, NK cells were isolated using the NK cell negative selection kit from Stem-Cell Technologies, according to the manufacturer's instructions. Purity of isolated cells was always >95%, as assessed by CD56 and CD3 costaining. For experiments with NK cell subsets, cells were isolated using fluorescence-activated cell sorting (FACS Aria, BD Biosciences). Cell lines were a gift from U. Zangemeister-Wittke (Institute of Pharmacology, University of Bern, Bern, Switzerland) and D. Stroka (Visceral and Transplantation Surgery, Department of Clinical Research, University of Bern, Bern, Switzerland).

mAbs and cell labeling. PBMCs, lymphocytes isolated from tissues or purified NK cells, were labeled using fluorescent mAbs directed against surface molecules (20 minutes at 4°C), washed in PBS with 0.2% BSA (Sigma-Aldrich), and acquired using a FACSCalibur or FACSVerse (BD Biosciences). Cells were labeled either directly ex vivo or, where indicated, after 30 minutes of treatment with 25 mU neuraminidase (Roche Diagnostics) at 37°C. Intracellular cytokine staining was done at 4°C for 30 minutes (see below). All mAbs were purchased from Biolegend, with the exception of anti-human Siglec-9, V450-conjugated anti-CD45, PerCP-conjugated anti-CD19, APC-conjugated anti-CD5, FITC-conjugated anti-IFN- γ , and PE-conjugated anti-MIP-1 β (BD Biosciences); anti-human Siglec-7 (Beckman Coulter); anti-human NKG2A and NKG2C (R&D Systems); and eFluor 450-conjugated anti-human TNF- α (eBioscience). Anti-human KLRG1 mAb was a gift from H. Pircher (Universitätsklinikum Freiburg, Freiburg, Germany). Each mAb was titrated on PBMCs before use. Data analysis was performed using FCS Express. Fab fragments of unlabeled anti-human Siglec-7 and -9 mAbs were produced by papain digestion and subsequent purification using a protein A-Sepharose column Fab preparation kit (Pierce Biotechnology) according to the manufacturer's instructions. Purity of the Fab fragments was confirmed by SDS-PAGE analysis.

Cell culture. All cell lines and purified human NK cells were cultured in RPMI medium (Sigma-Aldrich) supplemented with 10% FCS (Life Technologies) and complete medium (1% penicillin/streptomycin; Life Technologies). Cells were cultured for the indicated times in the presence of the cytokines rhIL-2 (100 U/ml; Proleukin, Roche Diagnostics), rhIL-8 (100 ng/ml; R&D Systems), rhIL-12 (50 ng/ml; Peprotech), rhIL-15 (50 ng/ml; Peprotech), rhIL-18 (100 ng/ml; Peprotech), and rhIL-21 (20 ng/ml; Peprotech).

Telomere length measurement by automated multicolor flow-FISH. For telomere length analysis, human NK cell subsets were isolated from the peripheral blood of 3 healthy donors by fluorescence-activated cell sorting as described above. Telomere length measurement by in situ hybridization and flow cytometry (automated multicolor flow-FISH) was as previously described (52). Briefly, 5.3×10^4 to 1×10^6 cells were used for in situ hybridization. Cells were incubated with 170 μ l hybridization mixture containing 75% deionized formamide (Sigma-Aldrich), 20 mM Tris (pH 7.1; Sigma-Aldrich), and 1% BSA (Sigma-Aldrich) with no probe (unstained) or 0.3 μ g/ml telomere-specific FITC-conjugated (C₃TA₂)₃ peptide nucleic acid (PNA) (Applied Biosystems). Denaturation was done at 87°C for 15 minutes, and hybridization was performed in the dark and at room temperature for 90 minutes. Excess and nonspecifically bound telomere PNA probe was removed by 4 wash steps at room temperature using 1 ml washing solution containing 75% formamide, 10 mM Tris, 0.1% BSA, and 0.1% Tween 20 (Sigma-Aldrich), followed by 1 \times 1 ml wash with a solution containing PBS, 0.1% BSA, and 0.1% Tween 20 at room temperature. DNA counterstaining was performed using a solution containing PBS, 0.1% BSA, and a subsaturating amount of LDS 751 (0.01 μ g/ml; Invitrogen) overnight. Acquisition of telomere fluorescence was performed using FACSCalibur (BD Biosciences). For each sample, unstained and telomere-stained samples were tested. FlowJo (Tree Star Inc.) was used for analysis of telomere length in the specific cell subsets. Specific telomere fluorescence was determined as the difference between the fluorescence of the stained samples minus the (auto-)fluorescence of the corresponding unstained sample. Using calibration beads and an internal standard of cow thymocytes, the telomere fluorescence was calculated into kilobases of telomere length.

Chemotaxis assay. Standard Transwell chemotaxis assay was performed with subsets of human NK cells highly purified by fluorescence-activated cell sorting (FACS Aria; BD Biosciences). In brief, medium supplemented or not with 1 nM rhIL-8 (R&D Systems) was added to the lower chamber of Transwell plates with 5- μ m pores (Costar Corning). NK cells were added to the upper chamber, and plates were incubated for 3 hours at 37°C. After incubation, equal volumes of CountBright bead (Invitrogen) solution were added to the migrated cells, and 3,500 beads were acquired per sample using a flow cytometer. The proportion of migrating cells was calculated by dividing the number of migrating cells by the total number and expressed as a percentage.

Proliferation assay. Purified NK cells were labeled with a final concentration of 5 μ M CFSE (Molecular Probes), according to the manufacturer's instructions. Cells were cultured in complete medium supplemented with rhIL-2 (400 U/ml; Roche Diagnostics) and rhIL-15 (50 ng/ml; Peprotech) in the presence of the indicated mAbs. CFSE fluorescence was evaluated at days 0, 6, and 9 on CD3⁺CD56⁺ cells by flow cytometry.

Survival assay. Purified NK cells were cultured in complete medium for 24 hours in the presence of the indicated mAbs. Percentage of surviving cells was evaluated by propidium iodide (Sigma-Aldrich) and annexin V (BD Biosciences) staining, as previously described (33, 53), or by using GFP-conjugated recombinant annexin V (gift from T. Kaufmann, University of Bern, Bern, Switzerland).

Killing assay. Cytolytic NK cell activity toward susceptible target cell lines K562 and 721.221 and nonsusceptible HeLa cells was assessed using a standard ⁵¹Cr release assay. Briefly, purified NK cells were cocultured at different E/T ratios with ⁵¹Cr-labeled cells, either untreated or neuraminidase treated, or in the presence or absence of Fab fragments or mAbs. After 4 hours, supernatants were collected, and ⁵¹Cr release was measured using a Top Count NXT microplate scintillator and luminance counter (Packard BioScience). Specific lysis was calculated as (experimental - spontaneous release)/(total - spontaneous release) and expressed as a percentage.



CD107a mobilization assay. For CD107a mobilization assay, purified human NK cells were incubated at a 1:1 ratio with target cell lines for 4 hours, in the presence of CD107a mAb (Biolegend) and the indicated stimuli. After incubation, cells were washed with PBS plus 0.2% BSA (Sigma-Aldrich) and analyzed on a FACSVerse (BD Biosciences). Where indicated, target cells were pretreated with 25 mU neuraminidase (Roche Diagnostics) for 30 minutes (or for 1 hour, in the case of HeLa) at 37°C and washed extensively before cocubation.

Intracellular staining of cytokines. 10⁵ resting NK cells were added to 10⁵ K562 cells in 200 µl complete medium. Target cells were treated with neuraminidase when needed. Cells were incubated for 1 hour at 37°C in 5% CO₂. Thereafter, Brefeldin A (GolgiPlug; Becton Dickinson) was added to the cultures, which were incubated for 5 more hours. After a total of 6 hours of incubation, cells were spun down and incubated with fluorochrome-conjugated mAbs for surface staining. Cells were then washed, fixed with 2% paraformaldehyde in PBS, permeabilized, and stained intracellularly with fluorochrome-conjugated mAbs against cytokines and chemokines. Finally, cells were washed and analyzed on a BD FACSVerse (BD Biosciences). Data were analyzed with FlowJo 10.0.6 software (Tree Star Inc.).

Cytokine secretion assay. Purified human NK cells were stimulated with rhIL-2 (Roche Diagnostics), rhIL-12 (Peprotech), and rhIL-18 (Peprotech) for 4 hours, in the absence or presence of mAbs. Supernatants were collected and analyzed using the human Th1/Th2 CBA Kit, the Inflammatory Cytokine CBA Kit, and IFN-α and GM-CSF Flex Sets (BD Biosciences).

Quantification of Siglec-7 and -9 ligands on tumor cells and primary melanocytes. Tumor cell lines were maintained in complete medium or DMEM (Invitrogen) supplemented with 10% FCS and 1% penicillin/streptomycin. Primary melanocytes were maintained in Medium 154 (Invitrogen) supplemented with human melanocyte growth supplement (HMGS) (Invitrogen) and 1% penicillin/streptomycin. Peripheral blood SSC^{lo}CD45^{lo} leukemia cells from AML patients and CD45⁺CD5⁺CD19⁺ cells from CLL patients were analyzed by flow cytometry. For Siglec ligand staining, recombinant human Siglec-hFc (R&D Systems) were mixed with PE-conjugated anti-human Ig (Jackson ImmunoResearch Laboratories) for 1 hour at 4°C before incubation with the cells for 30 minutes at 4°C. Where indicated, cells were pretreated with 25 mU neuraminidase (Roche Diagnostics) for 30 minutes at 37°C, or with 50 ng/ml rhTNF-α (R&D Systems) or 500 U/ml rhIFN-γ (gift from R. Dummer, Cancer Network Zurich, Zurich, Switzerland) for 24 hours. Fluorescent staining was analyzed using FACSCalibur.

Quantification of Siglec-7 and -9 ligands on paraffin-embedded tissue sections. Siglec ligand expression on paraffin-embedded tissue sections (6 µm) was assessed by immunofluorescence microscopy and lectin immunohistochemistry. For immunofluorescence studies, recombinant human Siglec-hFc (R&D Systems) were mixed with PE-conjugated anti-human Ig (Jackson ImmunoResearch Laboratories) for 1 hour at 4°C before use. Melan-A was detected using anti-human Melan-A mAb (clone A103; Dako) and secondary anti-mouse Alexa Fluor 488-labeled antibody (Invitrogen, Molecular Probes). Tissue sections were analyzed by confocal laser scanning microscopy (LSM 510; Carl Zeiss)

For immunohistochemical analysis, paraffin-embedded tissue sections were deparaffinized with NeoClear and graded ethanol. Antigen retrieval was performed by heating the sections in DAKO target retrieval solution (Dako) for 3 minutes in a microwave, with intermediate cooling incubations of 30 minutes. Endogenous peroxidase activity was blocked with DAKO endogenous dual enzyme block (Dako), and specific staining of Siglec-7 and -9 ligands was done with 5 and 3 µg/ml Siglec-hFc (R&D Systems), respectively, for 90 minutes at 37°C, or with human IgG1 (Sigma-Aldrich) as negative control. A biotinylated goat anti-human (Fab)² fragment (Jackson ImmunoResearch Laboratories) was used as secondary reagent. The complex was detected with streptavidin-conjugated horseradish peroxidase

(Dako) and visualized with Liquid DAB+ Substrate Chromogen System (Dako). All tissue sections were counterstained with hematoxylin. For morphologic analysis, an Axiovert 35 microscope (Carl Zeiss) was used.

Mice. NSG (NOD/LtSz-SCID IL-2Rγ^{null}) mice were obtained from the Jackson Laboratory and maintained at the Institute of Experimental Immunology of University of Zurich under specific pathogen-free conditions. Newborn NSG mice were irradiated with 100 cGy using a Cs source. 5–6 hours after irradiation, mice were injected intrahepatically with 1 × 10⁵ CD34⁺ human hematopoietic progenitor cells derived from human fetal liver tissue (obtained from Advanced Bioscience Resources). Preparation of human fetal liver tissue and isolation of human CD34⁺ cells was done as described previously (32, 54). Reconstitution of human immune system components in mice (i.e., huNSG mice) was analyzed 10–12 weeks after engraftment and again before the start of experiments. Animals used in experiments were 4–5 month of age.

In vivo killing assay. K562 and HeLa target cells were labeled with 2 µM of the red fluorescent dye PKH26 (Sigma-Aldrich) according to the manufacturer's protocol and extensively washed. Half of PKH26-labeled cells were then treated with 50 mU neuraminidase (Roche Diagnostics) in RPMI plus 0.5% FCS for 30 minutes at 37°C; the other half were left untreated. After incubation with neuraminidase, target cells were stained with 1 µM CFSE (Molecular Probes), whereas untreated cells were labeled with 5 µM CFSE. In each case, cell populations were washed, and 1–2 × 10⁶ cells per population were injected i.p. into huNSG mice pretreated with 50 µg poly I:C (Invivogen) for 12 hours, as previously described (4). Cells were harvested after 12 hours by peritoneal lavage, pelleted, washed, and stained with antibodies against murine CD45 (Biolegend) and human NKp46 (BD Biosciences) for 30 minutes on ice. Acquisition of flow cytometric data was performed on a LSR Fortessa cytometer (BD Biosciences).

Statistics. Unless otherwise indicated, data represent mean ± SEM. Significance of the results was determined using 2-tailed Student's *t* test. A *P* values less than 0.05 was considered significant.

Study approval. All human studies were in accordance with the guidelines of – and approved by the cantonal ethical committees of – Bern, Lausanne, and Zurich, Switzerland. Written informed consent was received from participants prior to inclusion in the study. All animal protocols were approved by the cantonal veterinary office of the canton of Zurich, Switzerland (protocol nos. 116/2008 and 148/2011).

Acknowledgments

This work was supported in part by grants from the Swiss National Science Foundation (310030_135734); the Bernese Cancer League; the Novartis Foundation for Medical and Biological Research; and the Department of Clinical Research (DCR) Prize 2010, University of Bern (to S. von Gunten). C. Jandus received support by the Swiss National Foundation (PMPDP3_129022, Marie-Heim Vögtlin Program). M. Wehrli was funded by the Swiss National Science Foundation (323530-139174, MD-PhD Program). Research in the laboratory of C. Münz is supported by grants from the National Cancer Institute (R01CA108609), the Sassella Foundation (10/02), Cancer Research Switzerland (KFS-02652-08-2010), the Association for International Cancer Research (11-0516), the Sobek Foundation, Fondation Acteria, the Vontobel Foundation, the Baugarten Foundation, Novartis, KFSP^{MS} and KFSP^{HL}D of the University of Zurich, and the Swiss National Science Foundation (310030_143979 and CRSII3_136241). O. Chijioke is the recipient of a postdoctoral fellowship of the Deutsche Forschungsgemeinschaft (DFG) (CH 723/2-1). T. Démoulin was supported by the Marie-Curie Industry-Academia Partnerships and Pathways Project Replixcel (251420) from the Seventh Framework Programme of the European Union.



P. Romero was funded in part by the Swiss National Science Foundation (310030_130812 and CRSII3_141878). We thank patients and healthy donors for blood donation and Bruce S. Bochner (Johns Hopkins University School of Medicine, Baltimore, Maryland, USA) for critical review of the manuscript.

Received for publication September 4, 2013, and accepted in revised form December 19, 2013.

Address correspondence to: Stephan von Gunten, Institute of Pharmacology, University of Bern, Friedbühlstrasse 49, CH-3010 Bern, Switzerland. Phone: 41.31.632.32.98; Fax: 41.31.632.49.94; E-mail: stephan.vongunten@pki.unibe.ch.

Camilla Jandus's present address is: Translational Tumor Immunology Group, Ludwig Center for Cancer Research, University of Lausanne, Lausanne, Switzerland.

1. Varki NM, Varki A. Diversity in cell surface sialic acid presentations: implications for biology and disease. *Lab Invest.* 2007;87(9):851–857.
2. Hakomori S. Tumor malignancy defined by aberrant glycosylation and sphingo(glyco)lipid metabolism. *Cancer Res.* 1996;56(23):5309–5318.
3. Kannagi R, et al. Altered expression of glycan genes in cancers induced by epigenetic silencing and tumor hypoxia: Clues in the ongoing search for new tumor markers. *Cancer Science.* 2010; 101(3):586–593.
4. Cazet A, Julien S, Bobowski M, Burchell J, Delanoy P. Tumor-associated carbohydrate antigens in breast cancer. *Breast Cancer Res.* 2010;12(3):204.
5. Fuster MM, Esko JD. The sweet and sour of cancer: glycans as novel therapeutic targets. *Nat Rev Cancer.* 2005;5(7):526–542.
6. Kannagi R, Izawa M, Koike T, Miyazaki K, Kimura N. Carbohydrate-mediated cell adhesion in cancer metastasis and angiogenesis. *Cancer Sci.* 2004; 95(5):377–384.
7. van Kooyk Y, Rabinovich GA. Protein-glycan interactions in the control of innate and adaptive immune responses. *Nat Immunol.* 2008;9(6):593–601.
8. Cohen M, et al. Sialylation of 3-methylcholanthrene-induced fibrosarcoma determines antitumor immune responses during immunoeediting. *J Immunol.* 2010;185(10):5869–5878.
9. Waldhauer I, Steinle A. NK cells and cancer immunosurveillance. *Oncogene.* 2008;27(45):5932–5943.
10. Nicoll G, Avril T, Lock K, Furukawa K, Bovin N, Crocker PR. Ganglioside GD3 expression on target cells can modulate NK cell cytotoxicity via siglec-7-dependent and -independent mechanisms. *Eur J Immunol.* 2003;33(6):1642–1648.
11. Daëron M, Jaeger S, Du Pasquier L, Vivier E. Immunoreceptor tyrosine-based inhibition motifs: a quest in the past and future. *Immunol Rev.* 2008;224(1):11–43.
12. Ravetch JV, Lanier LL. Immune inhibitory receptors. *Science.* 2000;290(5489):84–89.
13. Ljunggren HG, Kärre K. Host resistance directed selectively against H-2-deficient lymphoma variants. Analysis of the mechanism. *J Exp Med.* 1985;162(6):1745–1759.
14. Kärre K, Ljunggren HG, Piontek G, Kiessling R. Selective rejection of H-2-deficient lymphoma variants suggests alternative immune defence strategy. *Nature.* 1986;319(6055):675–678.
15. Nagler A, Lanier LL, Cwirla S, Phillips JH. Comparative studies of human FcR1-positive and negative natural killer cells. *J Immunol.* 1989; 143(10):3183–3191.
16. Jacobs R, et al. CD56bright cells differ in their KIR repertoire and cytotoxic features from CD56dim NK cells. *Eur J Immunol.* 2001;31(10):3121–3126.
17. Cooper MA, et al. Human natural killer cells: a unique innate immunoregulatory role for the CD56bright subset. *Blood.* 2001;97(10):3146–3151.
18. Falco M, et al. Identification and molecular cloning of p75/AIRM1, a novel member of the sialoadhesin family that functions as an inhibitory receptor in human natural killer cells. *J Exp Med.* 1999; 190(6):793–802.
19. Nicoll G, et al. Identification and characterization of a novel siglec, siglec-7, expressed by human natural killer cells and monocytes. *J Biol Chem.* 1999;274(48):34089–34095.
20. Belisle J, et al. Identification of Siglec-9 as the receptor for MUC16 on human NK cells, B cells, and monocytes. *Mol Cancer.* 2010;9(1):118.
21. Crocker PR, Paulson JC, Varki A. Siglecs and their roles in the immune system. *Nat Rev Immunol.* 2007; 7(4):255–266.
22. Varki A. Glycan-based interactions involving vertebrate sialic-acid-recognizing proteins. *Nature.* 2007;446(7139):1023–1029.
23. Jandus C, Simon HU, von Gunten S. Targeting siglecs – a novel pharmacological strategy for immuno- and glycotherapy. *Biochem Pharmacol.* 2011;82(4):323–332.
24. von Gunten S, Bochner BS. Basic and clinical immunology of Siglecs. *Ann N Y Acad Sci.* 2008; 1143:61–82.
25. Miyazaki K, et al. Colonic epithelial cells express specific ligands for mucosal macrophage immunosuppressive receptors siglec-7 and -9. *J Immunol.* 2012;188(9):4690–4700.
26. Ohta M, et al. Immunomodulation of monocyte-derived dendritic cells through ligation of tumor-produced mucins to Siglec-9. *Biochem Biophys Res Commun.* 2010;402(4):663–669.
27. Kawasaki Y, et al. Ganglioside DSGb5, preferred ligand for Siglec-7, inhibits NK cell cytotoxicity against renal cell carcinoma cells. *Glycobiology.* 2010;20(11):1373–1379.
28. Gieseke F, et al. Siglec-7 tetramers characterize B-cell subpopulations and leukemic blasts. *Eur J Immunol.* 2012;42(8):2176–2186.
29. Cohen M, Varki A. The sialome – far more than the sum of its parts. *OMICS.* 2010;14(4):455–464.
30. Kaneko Y, Nimmerjahn F, Ravetch JV. Anti-inflammatory activity of immunoglobulin G resulting from Fc sialylation. *Science.* 2006;313(5787):670–673.
31. Varki A, Angata T. Siglecs – the major subfamily of I-type lectins. *Glycobiology.* 2006;16(1):1R–27R.
32. Strowig T, et al. Human NK cells of mice with reconstituted human immune system components require preactivation to acquire functional competence. *Blood.* 2010;116(20):4158–4167.
33. von Gunten S, et al. Siglec-9 transduces apoptotic and non-apoptotic death signals into neutrophils depending on the pro-inflammatory cytokine environment. *Blood.* 2005;106(4):1423–1431.
34. Björkstöm NK, et al. Expression patterns of NKG2A, KIR, and CD57 define a process of CD56dim NK-cell differentiation uncoupled from NK-cell education. *Blood.* 2010;116(19):3853–3864.
35. Lopez-Vergès S, et al. CD57 defines a functionally distinct population of mature NK cells in the human CD56dimCD16+ NK-cell subset. *Blood.* 2010; 116(19):3865–3874.
36. Casilli F, et al. Inhibition of interleukin-8 (CXCL8/IL-8) responses by repertaxin, a new inhibitor of the chemokine receptors CXCR1 and CXCR2. *Biochem Pharmacol.* 2005;69(3):385–394.
37. Berahovich RD, Lai NL, Wei Z, Lanier LL, Schall TJ. Evidence for NK cell subsets based on chemokine receptor expression. *J Immunol.* 2006; 177(11):7833–7840.
38. Ito A, Handa K, Withers DA, Satoh M, Hakomori S. Binding specificity of siglec7 to disialogangliosides of renal cell carcinoma: possible role of disialogangliosides in tumor progression. *FEBS Lett.* 2001;498(1):116–120.
39. Yamaji T, Teranishi T, Alphey MS, Crocker PR, Hashimoto Y. A small region of the natural killer cell receptor, Siglec-7, is responsible for its preferred binding to α 2,8-disialyl and branched α 2,6-sialyl residues. A comparison with Siglec-9. *J Biol Chem.* 2002;277(8):6324–6332.
40. Levy MZ, Allsopp RC, Fitcher AB, Greider CW, Harley CB. Telomere end-replication problem and cell aging. *J Mol Biol.* 1992;225(4):951–960.
41. Pagès F, Galon J, Dieu-Nosjean MC, Tartour E, Sautès-Fridman C, Fridman WH. Immune infiltration in human tumors: a prognostic factor that should not be ignored. *Oncogene.* 2010;29(8):1093–1102.
42. Galon J, et al. Type, density, and location of immune cells within human colorectal tumors predict clinical outcome. *Science.* 2006;313(5795):1960–1964.
43. Romagné F, et al. Preclinical characterization of 1-7F9, a novel human anti-KIR receptor therapeutic antibody that augments natural killer-mediated killing of tumor cells. *Blood.* 2009;114(13):2667–2677.
44. Hamid O, et al. Safety and tumor responses with lambrolizumab (anti-PD-1) in melanoma. *N Engl J Med.* 2013;369(2):134–144.
45. Wolchok JD, et al. Nivolumab plus ipilimumab in advanced melanoma. *N Engl J Med.* 2013; 369(2):122–133.
46. Yuan J, et al. CTLA-4 blockade enhances polyfunctional NY-ESO-1 specific T cell responses in metastatic melanoma patients with clinical benefit. *Proc Natl Acad Sci USA.* 2008;105(51):20410–20415.
47. Koh CY, et al. Augmentation of antitumor effects by NK cell inhibitory receptor blockade in vitro and in vivo. *Blood.* 2001;97(10):3132–3137.
48. Curti A, et al. Successful transfer of alloreactive haploidentical KIR ligand-mismatched natural killer cells after infusion in elderly high risk acute myeloid leukemia patients. *Blood.* 2011; 118(12):3273–3279.
49. Maier S, et al. Inhibition of natural killer cells results in acceptance of cardiac allografts in CD28^{-/-} mice. *Nat Med.* 2001;7(5):557–562.
50. O'Reilly MK, Paulson JC. Siglecs as targets for therapy in immune-cell-mediated disease. *Trends Pharmacol Sci.* 2009;30(5):240–248.
51. von Gunten S, Simon HU. Cell death modulation by intravenous immunoglobulin. *J Clin Immunol.* 2010; 30(suppl 1):S24–S30.
52. Baerlocher GM, Vulto I, de Jong G, Lansdorp PM. Flow cytometry and FISH to measure the average length of telomeres (Flow FISH). *Nat Protoc.* 2006;1(5):2365–2376.
53. von Gunten S, Schaub A, Vogel M, Stadler BM, Miescher S, Simon HU. Immunological and functional evidence for anti-Siglec-9 autoantibodies in intravenous immunoglobulin (IVIg) preparations. *Blood.* 2006;108(13):4255–4259.
54. White RE, et al. EBNA3B-deficient EBV promotes B cell lymphomagenesis in humanized mice and is found in human tumors. *J Clin Invest.* 2012; 122(4):1487–1502.